

# Balloon studies of cosmic rays at the Lebedev Physical Institute, RAS

Yu I Stozhkov, V S Makhmutov, N S Svirzhevsky

DOI: <https://doi.org/10.3367/UFNe.2021.06.039215>

## Contents

1. Introduction	986
2. Equipment	988
3. 11- and 22-year cycles in cosmic rays	988
4. Magnetic fields in the heliosphere and processes determining the modulation of cosmic rays	989
5. What do experimental data show?	991
6. Conclusions	993
References	993

**Abstract.** Regular measurements of cosmic ray fluxes in the atmosphere have been performed at the Lebedev Physical Institute since 1957. These experiments are briefly described. In the atmosphere, secondary fluxes of charged particles are detected, which are mainly (more than 99%) produced by primary protons and nuclei. Long-term (11- and 22-year) changes in cosmic ray fluxes in the atmosphere produced by primary protons and nuclei and in primary electron fluxes are analyzed. Data on primary electrons are obtained using high-altitude balloons and satellites. The analysis shows that the time dependences of positively and negatively charged particles in the heliosphere have the same form, i.e., they are modulated in the same way. This result contradicts the generally accepted model of cosmic ray modulation in the heliosphere, which should be significantly modified.

**Keywords:** cosmic rays, solar activity, heliosphere, modulation

## 1. Introduction

The Dolgoprudny Scientific Station (DSS) was opened at the Lebedev Physical Institute, RAS (FIAN) according to the closed resolution no. 503-208, March 4, 1946, of the Council of People's Commissars. The text of the resolution was very short: "To organize a scientific station at the Lebedev Physics Institute, USSR Academy of Sciences, in the town of Dolgoprudny, Moscow region." The resolution was signed by I V Stalin, Chairman of the Council of People's Commissars. The creation of the station was initiated by Academician S N Vernov and supported by Academicians S I Vavilov and D V Skobeltsyn.

Yu I Stozhkov<sup>(a)</sup>, V S Makhmutov<sup>(b)</sup>, N S Svirzhevsky<sup>(c)</sup>  
 Lebedev Physical Institute, Russian Academy of Sciences,  
 Leninskii prosp. 53, 119991 Moscow, Russian Federation  
 E-mail: <sup>(a)</sup> stozhkovyi@lebedev.ru, <sup>(b)</sup> makhmutovvs@lebedev.ru,  
<sup>(c)</sup> svirzhevskyns@lebedev.ru

Received 18 April 2021

Uspekhi Fizicheskikh Nauk 192 (9) 1054–1063 (2022)

Translated by M N Sapozhnikov

At that time, the main task to be implemented by our state was the creation of an atomic weapon. For this reason, for the first decade, the researchers at the DSS investigated the properties of cosmic rays (CRs) and their interactions with nuclei of various elements. In these years, CRs were in fact the only source of high-energy particles for studying nuclear interactions. Rather heavy scientific instruments were launched into the atmosphere on garlands from meteorological balloons (Fig. 1). The results of measurements were transmitted by radio to ground-based reception centers. Scientific instruments were launched from the DSS, FIAN territory, in the region of the town of Osh in the south, and in the Indian Ocean from the deck of an ocean vessel. New information was obtained on the nature of cosmic rays, cross sections of their interaction with nuclei of air, etc. [1–8]. The head of this work, S N Vernov, was awarded the State Stalin Prize of the first degree for experimental investigations of CRs in the upper layers of the atmosphere.

Studies of modulation effects in CRs by the method of regular probing were initiated by S N Vernov and A N Charakhch'yan in the middle of 1957. This year was proclaimed the International Geophysical Year. A worldwide network of CR stations (mainly neutrons monitors) was

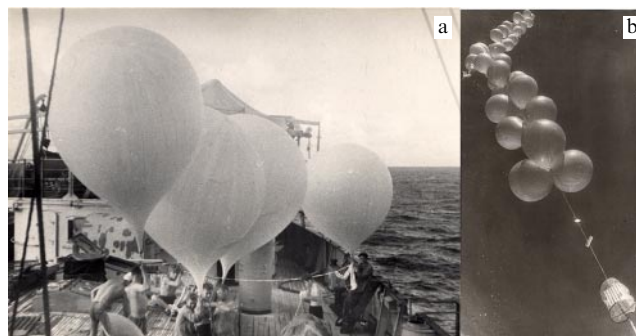


**Figure 1.** (a) Vityaz ship deck, Indian Ocean, 1949. Preparations for launching an instrument to study CR fluxes in the atmosphere. (b) Launching of scientific instruments. The instruments were launched to altitudes of 30–35 km using lines from aerologic balloons.

created for studying modulation effects. In the USSR, the network of CR stations, including neutron monitors and stations for probe CR measurements directly in the atmosphere, was created by S N Vernov. Since then, continuous measurements of CR fluxes and regular measurements of charged particles in the atmosphere have been performed, i.e., for 65 years.

The question can be raised: why should measurements of CRs in the atmosphere be performed at different latitudes (from polar to equatorial latitudes) and different altitudes (from Earth's surface up to 30–35 km)? The answer is that measurements at different latitudes use Earth's magnetic field to analyze particles over their energy or rigidity  $R_c$  ( $R_c = pc/(ze)$ , where  $R_c$  is the geomagnetic cutoff rigidity in gigavolts,  $p$  is the particle momentum,  $c$  is the speed of light,  $ze$  is the particle charge, and  $e$  is the electron charge). The geomagnetic field allows the existence of particles with the rigidity  $R \geq R_c$  at each point of observation on the atmosphere boundary. During motion from the pole to the equator, the value of  $R_c$  changes from 0 to 5–17 GV. Measurements performed at different latitudes allow us to study modulation effects of CRs in different energy intervals. On the other hand, Earth's atmosphere is itself a natural analyzer of particles over their energies. The lower is the altitude of measurements (i.e., the greater the atmospheric pressure), the higher the average effective energy of detected particles. For example, in polar regions, where  $R_c \approx 0$ , at altitudes of  $\sim 30$  km, protons with energies above 100 MeV are detected. On Earth's surface at the same latitude, to be detected by its secondary neutrons or secondary charged particles, a primary proton should have an energy above 1.5 GeV or above 9.0 GeV, respectively.

The next question is: why are long-term (several ten or hundred years) observations of CR fluxes needed? The answer to this question is quite simple: cosmic rays are strongly affected by solar activity, which varies with periods of  $\approx 11$ ,  $\approx 22$ , or  $\approx 90$  years and with longer periods. Sometimes, approximately once every 180 years, the Sun exhibits the deep minima of solar activity. Quite probably, we are at present in one of these minima. Because CRs play a significant role in atmospheric processes, atmospheric electricity, and global climate variation, it is necessary to have information on their fluxes in the atmosphere over long time intervals [9–13]. Our teachers, S N Vernov, A E Chudakov, and A N Charakhch'yan, understood the necessity of long-term CR measurements and supported these studies. Even in the crime-ridden 1990s, regular CR monitoring in the atmosphere did not cease. At that time, A E Chudakov was the chairman of the Scientific Council on the complex program Cosmic Rays, and only his support ensured regular CR probing in the atmosphere.

The long series of data on CR fluxes and solar activity provide a basis for understanding physical processes relating variations in cosmic rays with solar activity and characteristics of the solar plasma in the heliosphere, and give the opportunity to verify the correctness of theoretical concepts about CR modulation and the validity of theoretical predictions. The long series of homogeneous experimental data are used for physical (mathematical) simulations of 11- and 22-year variations of galactic cosmic rays (GCRs) and for studying the nature of other long-term trends in various indices of solar activity.

Note that long-term observations of various physical parameters are performed in many scientific fields. For

example, solar activity (the number of solar spots) has been regularly observed since 1740, the global temperature of the surface atmospheric layer has been measured since 1880, and the solar constant (the solar energy flux on Earth's orbit) has been studied since 1978. These long observation periods have provided the required quantitative information on variations in solar activity, global climate warming over several hundred years, and the change in the solar constant from the maximum to minimum of solar activity during the 11-year solar cycle.

Regular measurements of charge-particle fluxes in the atmosphere at altitudes up to 30–35 km were started in the northern polar regions (Murmansk region, the geomagnetic cutoff threshold is  $R_c = 0.5$  GV) and the Moscow region (town of Dolgoprudny, Moscow region,  $R_c = 2.4$  GV) in the middle of 1957. Later, such measurements were performed at the middle latitudes (Alma-Ata together with Kazakh University,  $R_c = 6.7$  GV, 1962–1990) and in Antarctica (Mirny Station,  $R_c = 0.04$  GV, from 1963 to the present). In the second half of the 20th century, long-term measurements (more than 10 years) of CR fluxes were performed in Tiksi (together with the Institute of Cosmophysical Studies and Aeronomy (IKFIA), Siberian Branch, USSR Academy of Sciences), Erevan (together with the Erevan Physics Institute, Armenian SSR Academy of Sciences), Norilsk (together with the Irkutsk station of the Institute of Earth Magnetism, the Ionosphere, and the Propagation of Radiowaves (IZMIRAN), Siberian Branch, USSR Academy of Sciences). In addition, the planetary distributions of fluxes of charged particles at different altitudes in the atmosphere were extensively studied. Radiosondes were launched from research vessels on the way from Leningrad to Antarctica and back [14–18].

Note that, at present, CRs are extensively studied at many laboratories in the world in a broad energy range from  $10^6$  to  $10^{21}$  eV. CR fluxes in the energy range of 0.1–30 GeV depend on the solar activity level and considerably decrease in the years of maximal solar activity. A certain contribution to the CR flux detected in the heliosphere is made by the Sun. Sometimes, the Sun exhibits high-power solar flares releasing huge energies of  $\sim 10^{32}$  erg, in which charged particles (mainly protons) are accelerated up to energies of  $\sim 20$  GeV.

Thus, CR studies include the investigation of the generation of CRs in sources, their propagation in the Galaxy and the Solar System, the generation of charged particles on the Sun, and their propagation in the near-Sun and interplanetary space.

Since the middle of 1957 till the present, researchers at the DSS, FIAN have launched more than 87 thousand CR radiosondes at different places on Earth. Unique homogeneous experimental data about the fluxes of charged particles at latitudes with different geomagnetic cutoff rigidities were obtained at different altitudes in the atmosphere.

Regular probing of fluxes of charged particles in Earth's atmosphere was used to study the following issues:

- (1) Long-term CR variations in the 11- and 22-year solar activity cycles and the relationship of these variations with parameters of solar activity and the interplanetary medium.
- (2) Short-term CR variations (27-day, 24-day variations, Forbush effects in CRs) and their relation to solar activity.
- (3) Detection of solar CR flares in the atmosphere, studies of acceleration mechanisms of particles in solar flares and processes of their propagation in the heliosphere.

(4) Precipitation of particles (electrons) from Earth's radiation belts to the atmosphere at high (and possibly middle) latitudes.

(5) Relation between charge-particle fluxes and characteristics of atmospheric electricity. Cosmic rays are the main source of electric charges (ions) in Earth's atmosphere.

(6) Role of charged-particle fluxes in atmospheric processes and in the change in Earth's climate. The importance of this area has become especially clear in the last two decades. At CERN, special CLOUD (Cosmics Leaving OUtdoor Droplets) experiments were performed for over 10 years (with the participation of researchers from the DSS, FIAN) for studying the role of CRs in atmospheric processes and climate variations.

(7) Operative control of the radiation situation in the atmosphere and registration of radioactive clouds.

Below, we will discuss long-term CR variations, in particular, the correctness of our concept of CR modulation in the heliosphere. Other questions, such as the nature of CRs, the propagation of CRs in the Galaxy, solar cosmic rays, and the precipitation of particles in Earth's atmosphere, are considered in [19–22].

## 2. Equipment

Cosmic ray flux measurements in the atmosphere were regularly performed at FIAN with a specially developed CR radiosonde (Fig. 2) and ground-based receiving equipment. During each flight of the radiosonde, charged-particle fluxes were measured at different altitudes in the atmosphere. Charged particles have been detected since the beginning of experiments till the present with STS-6 gas-discharge counters produced in our country. These detectors do not require a high-voltage power supply (the operating voltage of the counter is 380 V), have a high stability, and can operate for a few ten years. Before the 2000s, a radiosonde had two STS-6 counters forming a double-coincidence telescope. A 7-mm aluminum filter absorbing radioactive particles (natural or artificial) was placed between counters. Each charged particle entering the upper counter or passing thorough the telescope triggers a response in the electronics. A single counter detects CRs and radioactivity, while the telescope detects only CRs. Particles detected with a single counter or the telescope have different durations of radio signals [23]. The electronics forms the output pulse of a transmitter, sending it to a ground-based receiving unit. The ground-based receiving equipment separates these signals. At present, the radiosonde weighs 600–700 g (before the 1970s, the radiosonde weighed 2–3 kg). Researchers at the DSS, FIAN have fabricated about 500 radiosondes per year in the last two decades. From the beginning of the 2000s, because of financial difficulties, only one counter has been used in a radiosonde.

The receiving equipment consists of a P-313 AM receiver, oscilloscope, and computer. Output signals from the receiver fed to the computer have different durations: 300–500  $\mu$ s from the counter and 800–1000  $\mu$ s from the telescope. A special computer program separates these signals into two channels and averages the counting of each channel for the time  $\Delta t$ , usually equal to 1 min. When an atmospheric pressure sensor operates through certain intervals  $\Delta p$ , where  $p$  is the atmospheric pressure [ $\text{g cm}^{-2}$ ], the duration of signals from the telescope increases to  $\sim 1500 \mu$ s. Thus, the radiosonde transfers information over three channels: data from a single

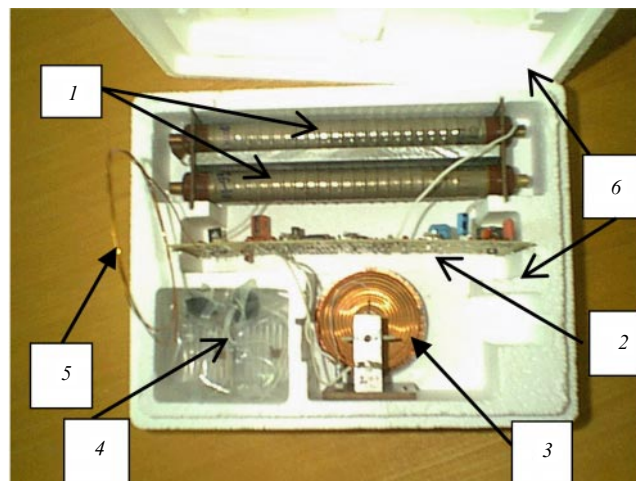


**Figure 2.** (Color online.) CR radiosonde developed by researchers at the DSS, FIAN: 1 — gas-discharge STS-6 counters, 2 — electronic setup with a 400-V voltage converter and a VHF transmitter, 3 — atmospheric pressure sensor, 4 — power supply batteries, 5 — VHF transmitter antenna, 6 — foam housing.

counter (radioactivity and CRs) (1st channel), telescope data (CRs) (2nd channel), and data from the atmospheric pressure sensor (3rd channel). Data from each radiosonde flight are recorded in the computer.

To obtain uniform series of experimental data for more than 65 years, a system to calibrate the counters and telescopes was developed (Fig. 3). After the introduction of corrections to the counting rate of a single counter and the telescope to the efficiency of these detectors, we can compare data obtained at the current moment with data obtained in the past. This is the concept of uniformity of long series of experimental data. Corrections for each counter and telescope used in radiosonde flights are introduced by the average counting of five control counters and five control telescopes.

## 3. 11- and 22-year cycles in cosmic rays

Cosmic ray fluxes in the heliosphere are controlled by solar activity. The most large-scale changes in solar activity occur during the 11-year solar cycle. In addition to the 11-year cycle, the 22-year magnetic cycle is observed on the Sun, which is distinctly manifested in CRs [24]. Below, we will consider long-term CR variations in the 11- and 22-year cycles of solar activity in more detail. This question is quite relevant today, when the Sun has probably entered another grand solar minimum. Such minima are observed once every  $\approx 180$  years. Their duration can reach a few ten years. For example, the Maunder minimum lasted from 1645 till 1710. In this period, solar spots were in fact absent on the Sun [25]. During the last two minima of solar activity in 2009 and 2020, the Sun was very quiet, and we detected the highest CR fluxes for the entire history of their observations (over 60 years). The high CR fluxes were observed with neutron monitors and on near-Earth spacecraft.

As for the 22-year solar magnetic cycle, approximately at the maximum of each 11-year solar cycle, the direction of magnetic fields in the polar caps of the Sun change to the opposite one. The solar magnetic field can be approximately considered a dipole during the almost entire 11-year cycle of



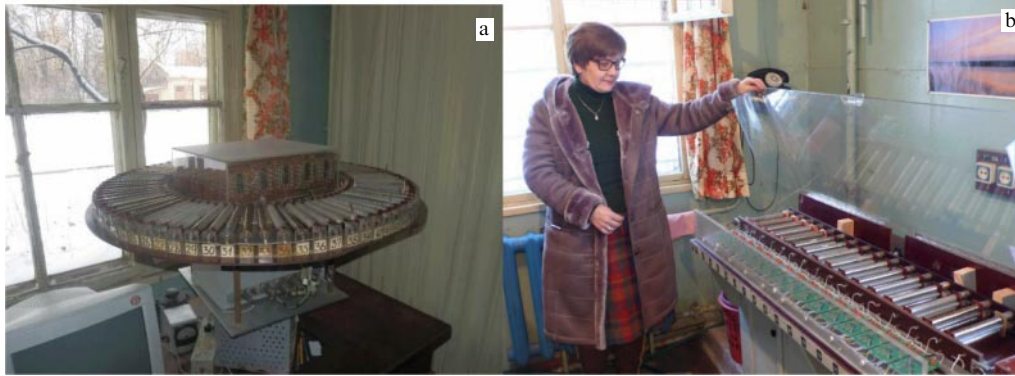


**Figure 3.** (Color online.) Devices for calibrating gas-discharge STS-6 counters (a) and double-coincidence telescopes (b). To obtain homogeneous radiation fields, the device for calibrating gas-discharge counters is rotated at a frequency of about three revolutions per minute.

solar activity, except 2–3 years of the solar activity maximum. The inversion of the solar polar magnetic field is followed by a change of signs of the magnetic field in the heliosphere. As shown below, the direction of magnetic fields on the Sun and in the heliosphere strongly affects CR fluxes.

Figure 4 shows the time dependences of CR fluxes (monthly average values) at the maximum  $N_m$  of their cascade curve in the atmosphere. The data were obtained at the north (Murmansk region) and south (Antarctica, Mirny Station) polar latitudes and at the middle north latitude (DSS, FIAN, Dolgoprudny, Moscow region). These data are presented on the FIAN site [26].

The time dependence of the CR flux exhibit several features. First, in 2009 and 2020, the highest levels of CR fluxes were detected for the entire period of their observation since 1957. These fluxes proved to be approximately 10–15% higher than those measured in May 1965 at the minimum of the 20-year solar activity cycle. Second, the 11-year CR cycles exhibit alternating spike and plateau shapes for time dependences of CR fluxes. Such an alternation in the solar-activity indices (for example, in the number of solar spots) is not observed. Different shapes of time dependences of CRs are caused by the 22-year solar magnetic cycle. The spike-shaped time dependence is observed in the negative phases of this cycle, when magnetic force lines come out of the south polar cap of the Sun and enter the north polar cap (denoted as  $A < 0$ ). The plateau-shaped time dependence is observed in the positive phases of the magnetic cycle, when magnetic force lines come out of the north polar cap and enter the south polar cap ( $A > 0$ ). In negative phases ( $A < 0$ ), the rotation axis  $\Omega$  of the Sun is directed oppositely to the dipole component  $\mathbf{M}$  of the solar magnetic field, i.e.,  $\Omega \uparrow \downarrow \mathbf{M}$ . In positive phases ( $A > 0$ ),  $\Omega \uparrow \uparrow \mathbf{M}$ .

Figure 5 shows the time dependence of CR fluxes with the rigidity  $R = 0.73–2.4$  GV (for protons with energies of 250–1500 MeV). These data are the differences among the points of the green and red curves in Fig. 3.

The spike-shaped and plateau-shaped time dependences of CR fluxes in the negative and positive phases of the 22-year solar magnetic cycle in periods of the solar-activity minima and near these periods are presented in Fig. 6. Different shapes of these dependences are distinctly observed.

Note that the change in the phase (inversion) of the solar magnetic cycle occurs in or near the solar activity maximum. The inversions of magnetic fields in the north and south polar caps of the Sun can begin and end at different times. A new

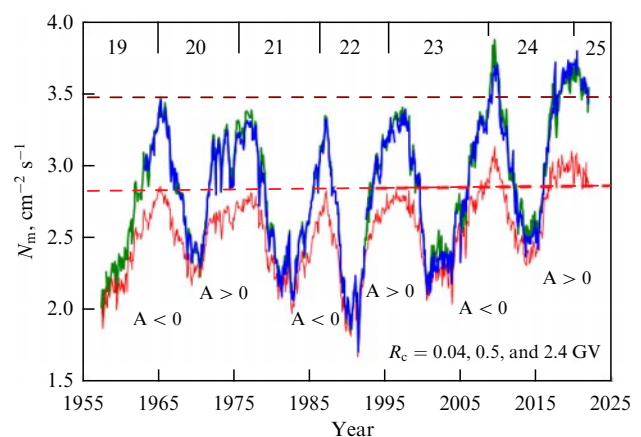


**Figure 4.** (Color online.) Time dependence of CR flux (monthly average values) at maximum  $N_m$  of their absorption curve in the atmosphere. Data obtained at the north (green curve,  $R_c = 0.5$  GV) and south (blue curve, Antarctica,  $R_c = 0.04$  GV) polar latitudes, and also at the middle north latitude (red curve,  $R_c = 2.4$  GV). Dashed brown and red straight lines are drawn through the maximum of CR fluxes observed in 1965. Numbers 19–25 at the top of the figure denote numbers of 11-year solar cycles.  $A > 0$  corresponds to the positive phase of the 22-year solar magnetic cycle,  $A < 0$  corresponds to the negative phase (see text).

solar cycle begins during the minimum of solar activity. Spots of the new 11-year solar-activity cycle appear at high heliolatitudes ( $\varphi \approx 30^\circ$ ) and then descend during development to lower latitudes ( $\varphi \approx 10^\circ$ ).

#### 4. Magnetic fields in the heliosphere and processes determining the modulation of cosmic rays

Data presented in Figs 3–6 show that the time dependences of CR fluxes alternate, going from the spike-shaped dependences for  $A < 0$  to the plateau-shaped dependences for  $A > 0$ . The period of such variations is approximately 22 years. A question arises as to the physical reason of such CR variations.

It is known that CRs propagating in the heliosphere from its boundary to Earth's orbit undergo diffusion, convection, adiabatic deceleration (the last is related to the expansion of solar wind with a magnetic field frozen in it), and drifts in a quasi-regular solar magnetic field [27–30]. In the heliosphere, two types of magnetic drifts take place, namely, gradient

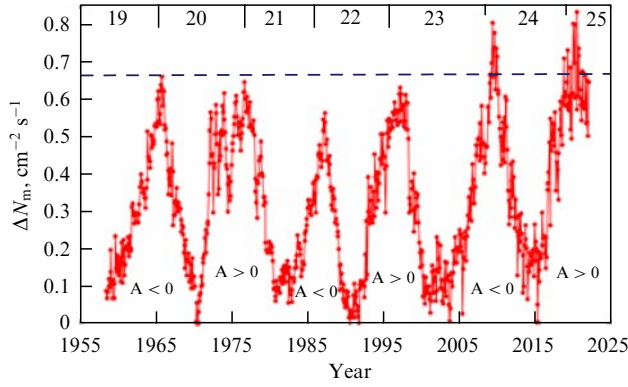


**Figure 5.** (Color online.) Timed dependence of CR flux at the maximum of its cascade curve in the atmosphere (secondary particles from primary CRs with rigidity  $R = 0.73\text{--}2.4$  GV). Notations as in Fig. 4.

magnetic drift with velocity  $\mathbf{v}_g$  and centrifugal drift with velocity  $\mathbf{v}_c$  [28, 29]. Formulas describing these phenomena have the form

$$\mathbf{v}_g = \frac{\alpha^2 \omega_B}{2B^2} [\mathbf{B} \times \nabla B], \quad \mathbf{v}_c = \frac{c\gamma m}{q} \frac{(v_{\parallel})^2 [\mathbf{r} \times \mathbf{B}]}{R^2 B^2},$$

where  $\alpha$  is the pitch angle of a particle,  $B$  is the induction of the interplanetary magnetic field (IMF),  $\mathbf{r}$  is the radius of curvature of an IMF force line,  $q$  is the particle charge,  $m$  is the particle mass,  $c$  is the speed of light,  $\gamma$  is the Lorentz factor, and  $\omega_B = qB/(\gamma mc)$  is the cyclotron frequency of a particle in magnetic field  $B$  [29, 30].

Among all the four above-mentioned processes controlling the motion of particles in the heliosphere, only drifts depend on the sign of a particle charge. Therefore, it is reasonable to assume that it is namely the drifts of particles

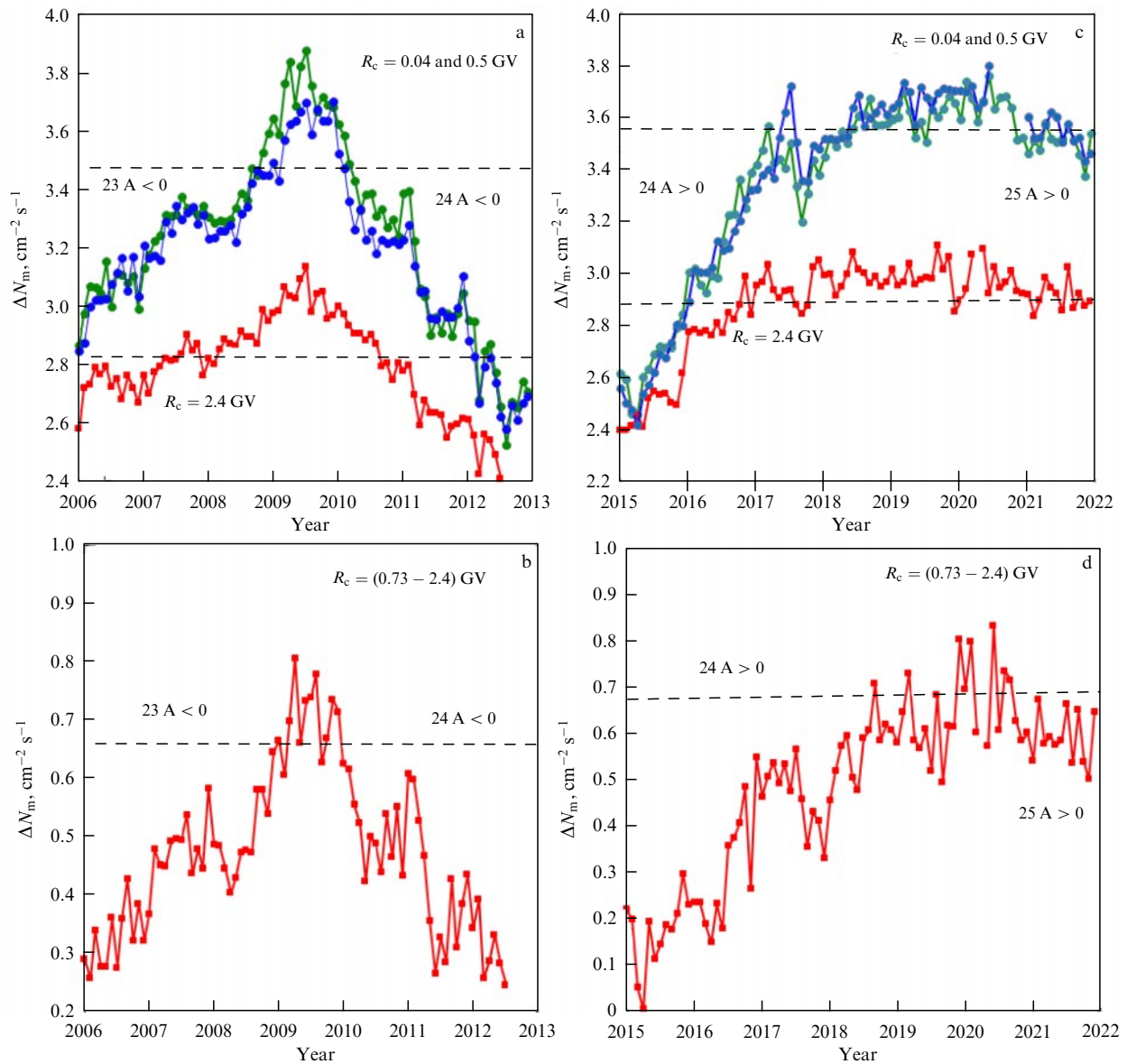


**Figure 6.** (Color online.) Monthly average time dependences of CR fluxes at the maximum of their cascade curves in the atmosphere at the minima and near minima of solar activity in the negative ( $A < 0$ ) (a, b) and positive ( $A > 0$ ) (c, d) phases of the 22-year solar magnetic cycle. (a, c) Data on CR fluxes obtained at north polar latitudes (green curve,  $R_c = 0.5$  GV), in Antarctica (blue curve,  $R_c = 0.04$  GV), and at the middle north latitude (red curve,  $R_c = 2.4$  GV). (b, d) CR fluxes produced in the atmosphere by primary protons and nuclei with rigidities of  $0.73\text{--}2.4$  GV. Numbers 23, 24, and 25 denote the numbers of 11-year solar cycles. For comparison, dashed straight lines show CR fluxes measured in the atmosphere in 1965.

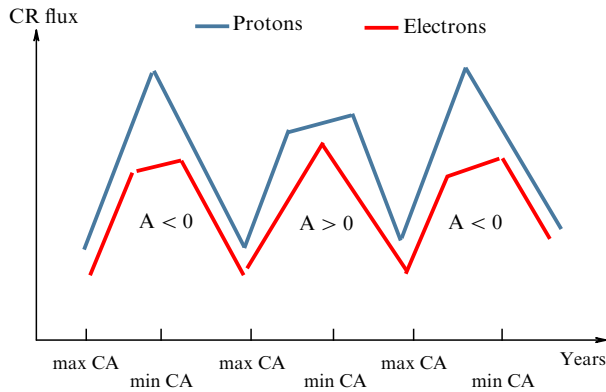


**Figure 7.** (Color online.) Schematic view of the expected time dependence of CR particles with a positive charge (protons and nuclei, blue curve) and electrons (red curve) in the negative ( $A < 0$ ) and positive ( $A > 0$ ) phases of the 22-year solar magnetic cycle. Notations ‘max SA’ and ‘min SA’ corresponds to periods of the maxima and minima of solar activity. Time interval between subsequent max SA (min SA) is about 11 years.

in a spiral IMF that are responsible for the two different forms of time dependences of CR fluxes (see Figs 3–5).

The generally accepted types of modulation of positive particles (protons and nuclei) and negative particles (electrons) in the heliosphere is shown schematically in Fig. 7. One can see that, in the 22-year solar magnetic cycle, protons and nuclei have the spike time dependence in negative phases ( $A < 0$ ) (blue curve), while electrons should have the plateau time dependence (red curve). In positive phases ( $A > 0$ ), the situation is the opposite [28].

According to the accepted concepts, the difference in the expected behavior among particles in CRs with opposite signs of the electric charge is caused by the fact that, in the heliosphere, for  $A < 0$ , the drift fluxes of protons and nuclei are directed from low heliolatitudes (from the heliospherical current sheet (HCS) to high latitudes, while electron drift fluxes are directed from high to low heliolatitudes (to the HCS). For  $A > 0$ , the situation becomes the opposite: the drift fluxes of protons and nuclei are directed from high to low heliolatitudes (to the HCS), while electron drift fluxes are directed from low to high heliolatitudes (from the HCS).

The relation of directions of magnetic fields in polar caps on the Sun and in the heliosphere and directions of drift currents for protons and electrons is schematically shown in Figs 8a, b: the positive phase of the 22-year solar magnetic cycle ( $A > 0$ ) (Fig. 8a) and the negative phase ( $A < 0$ ) (Fig. 8b). The dashed and solid vertical arrows show the directions of the rotation axis  $\Omega$  of the Sun and its dipole magnetic moment  $\mathbf{M}$ , respectively. In positive phases,  $\Omega \uparrow \uparrow \mathbf{M}$ , while in the negative phases,  $\Omega \uparrow \downarrow \mathbf{M}$ . Directions of the drift currents of particles with electric charge  $q > 0$  are shown by straight arrows to the left of the Sun, and, for particles with  $q < 0$ , to the right of the Sun (dashed arrows). Figures 8c, d show the expected time dependences for particles with  $q > 0$  (protons and nuclei) and  $q < 0$  (electrons) in positive and negative phases of the solar magnetic cycle. According to the drift theory, the time dependences for CR particles with opposite electric charges have different shapes. This difference is distinctly demonstrated by the ratio of the flow of particles with  $q > 0$  to the flow of particles with  $q < 0$  (Figs 8e, f).

The transport equation describing the motion of particles in the heliosphere does not have an analytic solution and is

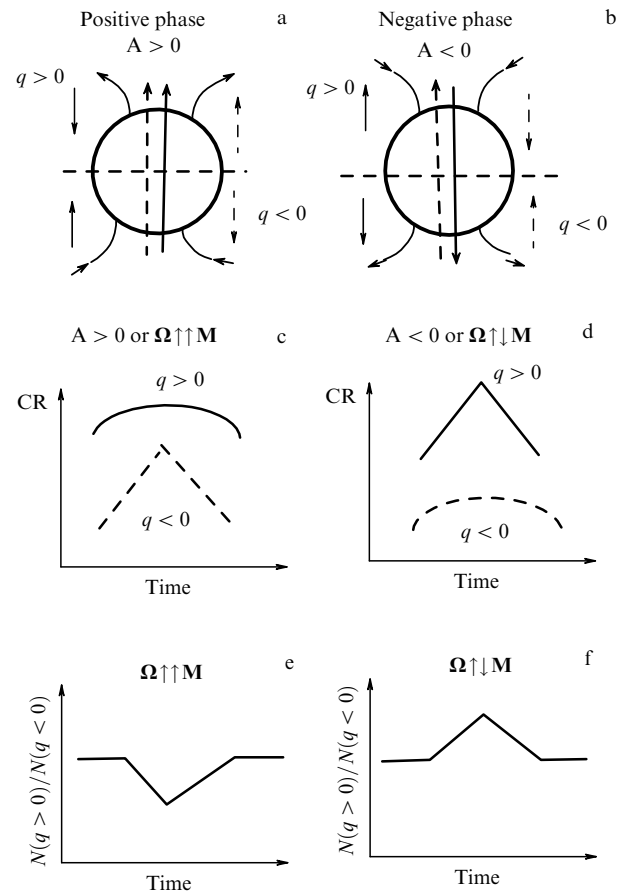


**Figure 8.** (a, b) Schematic view of the 22-year solar magnetic cycle in its positive ( $A > 0$ ) phases (a) and negative ( $A < 0$ ) phases (b). Circle denotes the Sun, curves with arrows show the direction of the solar magnetic field in polar caps on the Sun and in the heliosphere. Dashed and solid arrows in the circle denote the rotation axis  $\Omega$  of the Sun and direction of its dipole magnetic moment  $\mathbf{M}$ , respectively. In positive phases ( $A > 0$ ), these vectors have the same direction,  $\Omega \uparrow \uparrow \mathbf{M}$ , while in negative phases ( $A < 0$ ), they have opposite directions,  $\Omega \uparrow \downarrow \mathbf{M}$ . Directions of drift CR currents in the north and south parts of the heliosphere are shown by vertical arrows. Solid arrows in Fig. 8a correspond to particles with  $q > 0$ , and dashed arrows in Fig. 8b correspond to particles with  $q < 0$ . (c, d) Time dependences of CR particle flux in Earth's orbit with electric charges  $q > 0$  and  $q < 0$  in the positive ( $A > 0$ ) and negative ( $A < 0$ ) phases of this cycle according to the drift theory. (e, f) Time dependences of the  $N(q > 0)/N(q < 0)$  ratio of the proton, nuclear flux to the electron flux in the positive ( $A > 0$ ) and negative ( $A < 0$ ) phases of the 22-year solar magnetic cycle.

solved by numerical methods. The equation contains many parameters which can be selected to describe the spike-shaped and plateau-shaped time dependences of proton and nuclear fluxes in CRs according to the scenario described above [28].

## 5. What do experimental data show?

Currently, the scope of experimental data obtained for electrons is great enough, and it is possible to compare the time dependences of CR fluxes with electric charges of opposite signs. This is illustrated in Fig. 9. The red curve shows the time dependence for secondary CRs produced by protons and nuclei with rigidity  $R = 0.7\text{--}2.5$  GV [26]. The difference between particle fluxes measured at the maximum of transition curves in the atmosphere at polar latitudes and



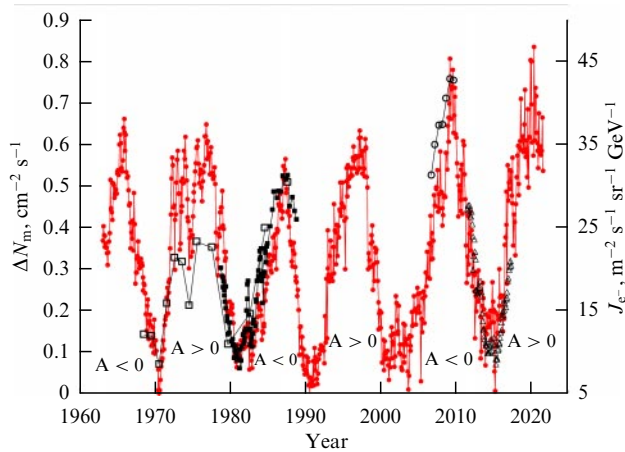


**Figure 9.** (Color online.) Time dependence of secondary particle flux  $I$  the atmosphere produced by primary CRs with rigidities of 0.73–2.5 GV (monthly average values, red dots, left axis) [26]. Electron flux is shown by black symbols (right axis). Light squares correspond to electrons with  $R_e = 0.9–1.1$  GV obtained with balloons [29]; shaded squares correspond to electrons with rigidities  $R_e = 0.9–1.1$  GV obtained with a satellite [29]; circles correspond to electrons with  $R_e = 0.9–1.1$  GV (PAMELA experiment [31]); triangles correspond to electrons with  $R_e = 1.0–1.2$  GV (AMS-2 spectrometer on the International Space Station) [32].

those at the middle latitude (see Fig. 4) gives the particle flow in the rigidity interval presented above. Figure 9 also shows electron fluxes with a rigidity of 1.0–1.1 GV obtained at different times with balloons (squares), satellites (shaded squares), and, in the last two decades in the cosmic PAMELA (Payload for Antimatter Matter Exploration and Light-Nuclei Astrophysics) experiment (circles) and AMS-2 (Alpha Magnetic Spectrometer 02) experiment (triangles).

A comparison of the time dependences of CR fluxes with  $q > 0$  and  $q < 0$  shows that these dependences have the same shape. Indeed, in the period from 06.1972 to 06.1977, a plateau was observed for both protons and electrons. The spike-shaped time dependences for these particles were observed in the mid-1980s and in 2008–2010. This result contradicts the conclusion of the drift theory that particles with opposite electric charges are modulated differently. These data suggest that the modulation of particles with electric charges of opposite signs in the heliosphere occurs in the same way [33]. Note that the authors of [34] made the opposite conclusion.

The presence of spiked and plateaued time dependences of the CR flux is probably not related to drift currents. A possible explanation for these shapes is presented below. The same time dependences for particles with electric charges of the opposite sign in the 22-year solar magnetic cycle do not deny the existence of drifts.

To explain qualitatively the two different shapes of the time dependence of the CR flux in periods with  $A > 0$  and  $A < 0$ , we will use the hypothesis about the existence of open and closed heliospheres proposed in [35, 36].

It is assumed that, during negative phases of the 22-year solar magnetic cycle ( $A < 0$  and  $\Omega \uparrow \downarrow \mathbf{M}$ ), the reconnection of magnetic force lines of the heliospheric and galactic magnetic fields occurs. The reconnection occurs at distances of  $\sim 100$  au at heliolatitudes above the spot-formation zone, i.e., at heliolatitudes  $\lambda > 10–15^\circ$ . Within approximately four years after the reconnection of the solar magnetic field (after the solar activity maximum), the solar spot-formation region

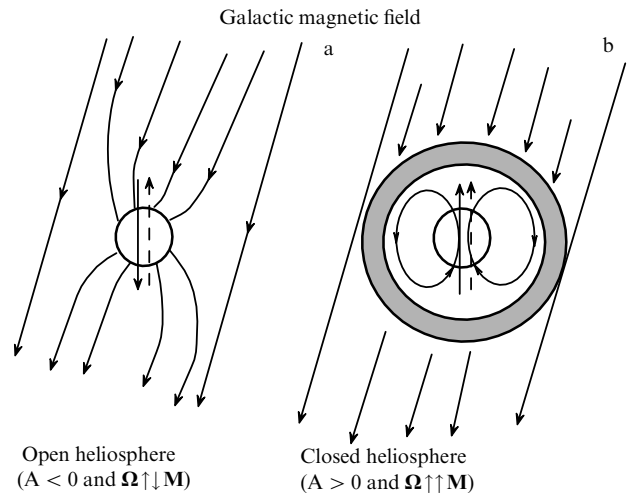


**Figure 10.** Schematic view of open (a) and closed (b) heliospheres. Sun is at the center. Dashed arrow is its rotation axis  $\Omega$ , solid arrow is the dipole magnetic moment  $\mathbf{M}$  of the Sun. Grey ring in panel b shows the region where the reconnection of the solar and galactic magnetic fields is absent and a magnetic barrier for CRs appears.

descends to heliolatitudes  $\lambda \approx 10–12^\circ$ . Outside this region, reconnection can occur. An open heliosphere is formed and CR particles can enter the heliosphere quite rapidly. This process is schematically shown in Fig. 10a.

In the positive phase of the 22-year solar magnetic cycle ( $A > 0$  and  $\Omega \uparrow \uparrow \mathbf{M}$ ), the reconnection of magnetic force lines of the heliospheric and galactic magnetic fields on the heliosphere boundary is absent (closed heliosphere) (Fig. 10b). On this boundary, a fairly thick (a few tens of astronomical units (au)) spherical magnetic barrier is formed. It is possible that the magnetic barrier occupies a region from the inner shock wave (termination shock,  $r \approx 85$  au) to heliopause ( $r \approx 125$  au) [37]. Cosmic ray particles diffuse through this barrier quite slowly, producing the plateau-shape of the time dependence of CR fluxes in Earth's orbit for protons, nuclei, and electrons.

Note that, at the minimum of the 24th solar cycle (2008–2010) and at the minimum of the 25th solar cycle (2019–2021), the solar polar magnetic field was weak compared to that observed at the previous minima of solar activity [38]. For this reason, the effect of a magnetic barrier (the absence of the reconnection of magnetic fields) in the time dependence of CRs in the last positive phase of the 22-year solar magnetic cycle (2013–2015) was less distinct. This can be seen, for example, in Fig. 4 by comparing CR plateaus observed in periods from 1974 to 1977 and from 2019 to 2021.

Large-scale modulation effects in CRs are related to the reconstruction of magnetic fields on the Sun and in heliosphere. Figure 11 shows the time dependences of electron and positron fluxes. The data are taken from [32]. The 2011–2015 period is related to the increasing branch of solar activity of the 24th 11-year cycle, when a decrease in the CR cycle was observed. The 2011–2013 period corresponds to the negative phase of the 22-year solar magnetic cycle ( $A < 0$ ). The configuration of the magnetic field in the heliosphere at that time was stable, the drift velocity of electrons was directed from high heliolatitudes to a heliospheric current layer, while the drift velocity of positrons (protons and nuclei) was directed vice versa, from the HCS to high heliolatitudes. The positron flux  $J_{e^+}$  for this period is normalized with respect to

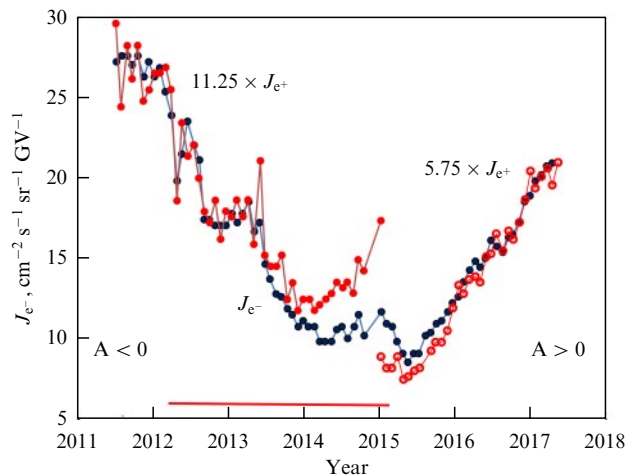


Figure 11. (Color online.) Time dependence of positrons (red dots) and electrons (black dots) with rigidity  $R_c = 1.01 - 1.22$  GV [32]. Positron flux is normalized to the electron flux (see text). Horizontal red straight line shows the inversion period of polar magnetic fields on the Sun.

the electron flux  $J_{e-}$ :  $J_{e-} = \kappa J_{e+}$ . The value  $\kappa = 11.2$  was calculated over the 2011.5–2013.3 time interval. One can see that the time dependences of electron and positron fluxes occur synchronously from mid-2011 to mid-2013.

The period from 2015 to 2018 corresponds to the solar activity decrease and the positive phase of the 22-year solar magnetic cycle ( $A > 0$ ). In this period, an increase in CR fluxes was observed. The positron flux was also normalized to the electron flux,  $J_{e-} = \kappa_1 J_{e+}$ . The value  $\kappa_1 = 5.75$  was calculated over the 2017.0–2017.4 time interval. One can see from Fig. 11 that the electron and positron fluxes change synchronously in time from the end of 2015 to mid-2017. In that period, the configuration of the magnetic field in the heliosphere was stable, but directions of drift currents changed to the opposite ones compared to the 2011–2013 period: the drift current of positrons was directed from high heliolatitudes to the HCS, while the drift current of electrons, on the contrary, was from the HCS to high heliolatitudes. Positron fluxes began to grow faster than electron fluxes.

In 2012, the inversion of the magnetic field on the Sun began [38, 39]. The duration of the inversion of the solar polar magnetic field is shown in Fig. 11 by the horizontal line. In the north polar cap of the Sun, this process took almost three years (beginning of 2012–beginning of 2015). In the south polar cap, the inversion occurred rather rapidly in May 2013 [38].

After the beginning of inversion on the Sun (after approximately a year, from mid-2013), the reconstruction of magnetic fields in the heliosphere began, which ended in November 2015. The heliosphere extends up to the heliopause ( $r \approx 120$  au), after which the interstellar medium begins. For solar wind with a magnetic field frozen to it to reach the heliopause, approximately a year is required.

In the heliosphere after the end of the magnetic field reconstruction, a new configuration of the magnetic field was established, and the heliosphere became closed ( $A > 0$ ). The directions of drift currents changed to the opposite ones: the drift current of positrons was directed from high heliolatitudes to the HCS, while the drift current of electrons, on the contrary, went from the HCS to high heliolatitudes. Positron fluxes began to grow faster than electron fluxes.

Data presented in Fig. 11 show that electron and positron fluxes (the latter are normalized with respect to electron fluxes in 2011) began to diverge in mid-2013. This occurred within approximately a year after the beginning of the magnetic field inversion in the north polar latitudes of the Sun (at the beginning of 2012) when CRs began to ‘feel’ the reconstruction of magnetic fields in the heliosphere. The magnetic field inversion on the Sun ended at the beginning of 2015, while the reconstruction in the heliosphere, at the end of 2015. Before the beginning and after the end of the inversion of magnetic fields in the heliosphere (mid-2013 and end of 2015, respectively), the time dependences of electron and positron fluxes are similar. During the reconstruction of heliospheric magnetic fields (mid-2013 and end of 2015, respectively), electrons and positrons behave differently.

## 6. Conclusions

Experimental data on CRs obtained from measurements in the atmosphere and data on electrons (balloon and satellite measurements) are analyzed. In the atmosphere, secondary charged particles produced by protons and nuclei, i.e., by cosmic particles with positive electric charges, were measured. It is shown that particles with opposite electric charges are modulated by solar activity in the same way. In positive phases of the 22-year solar magnetic cycle, the time dependences of particles of both signs have a plateau-shaped character in the minimum of the solar activity and near it for approximately four years. In negative phases of the solar magnetic cycle, a spike-shaped time dependence is observed for particles of both signs.

This effect is explained by assuming that, during negative phases of the 22-year solar magnetic cycle ( $\Omega \uparrow \downarrow \mathbf{M}$ ), the reconnection of magnetic force lines of galactic and solar magnetic fields occurs, and the heliosphere becomes open. Cosmic rays freely penetrate into it, and the spiked time dependence of CR particles is observed independently of their electric charge. In positive phases of the magnetic cycle on the Sun ( $\Omega \uparrow \uparrow \mathbf{M}$ ), the reconnection is absent and the heliosphere is closed to CRs. To enter the heliosphere, cosmic particles must overcome a diffusion magnetic barrier. This barrier gives the plateau-shaped time dependence of the CR flux independently of the sign of the electric charge of particles.

## Acknowledgments

Experimental data on CRs in Earth’s atmosphere presented in this paper were obtained by two generations of researchers, engineers, and technicians. The authors are grateful to them all.

## References

1. Briker S I et al. *Dokl. Akad. Nauk SSSR* **57** 141 (1947)
2. Vernov S N, Kulikov A M *Dokl. Akad. Nauk SSSR* **61** 1013 (1948)
3. Baradzei L T, Vernov S N, Smorodin Yu A *Dokl. Akad. Nauk SSSR* **62** 465 (1948)
4. Vernov S N, Grigorov N L, Charakhch’yan A N *Vestn. Mos. Gos. Univ.* (11) 71 (1949)
5. Alekseeva K I, Vernov S N *Dokl. Akad. Nauk SSSR* **69** 317 (1949)
6. Grigorov N L, Evreinova I M, Sokolov S P *Dokl. Akad. Nauk SSSR* **81** 379 (1951)
7. Alekseeva K I, Grigorov N L *Dokl. Akad. Nauk SSSR* **115** 259 (1957)
8. Grigorov N L et al. *Sov. Phys. Usp.* **23** 426 (1980); *Usp. Fiz. Nauk* **131** 521 (1980)
9. Stozhkov Yu I et al. *Nuovo Cimento C* **18** 335 (1995)



10. Stozhkov Yu I et al. *Geomagn. Aeron.* **36** (4) 211 (1996)
11. Ermakov V I Stozhkov Y I, in *Proc. of the 11th Intern. Conf. Atmospheric Electricity, Guntersville, Alabama* (NASA/CP-1999-209261, Ed. H J Christian) (Guntersville, AL: NASA, 1999) p. 242
12. Ermakov V I, Stozhkov Yu I “Mekhanizm obrazovaniya elektrichestva grozovykh oblakov” (“Mechanism of the thundercloud electricity production”), Preprint No. 25 (Moscow: Lebedev Physical Institute, RAS, 2002)
13. Stozhkov Y I *J. Phys. G* **29** 913 (2003)
14. Babarykin V K et al. *Geomagn. Aeron.* **4** (3) 485 (1964)
15. Stozhkov Yu I, Charakhch'yan A N, in *Antarktika* (Antarctica) Issue 10 (Moscow: Nauka, 1971) p. 16
16. Golenkov A E et al. *Trudy Fiz. Inst. Akad. Nauk SSSR* **122** 3 (1980)
17. Shea M A et al., in *Proc. of the 20th Intern. Cosmic Ray Conf., Moscow, 1987* Vol. 4 (Moscow: Nauka, 1987) p. 201
18. Golenkov A E et al., in *Proc. of the 21st Intern. Cosmic Ray Conf., Adelaide, Australia, 1990* Vol. 7 (Adelaide: Physics Publ. Univ. Adelaide, 1990) p. 14
19. Ptitsyna K V, Troitsky S V *Phys. Usp.* **53** 691 (2010); *Usp. Fiz. Nauk* **180** 723 (2010)
20. Panasyuk M I, Miroshnichenko L I *Phys. Usp.* **65** 379 (2022); *Usp. Fiz. Nauk* **192** 413 (2022)
21. Bazilevskaya G A et al. *J. Geophys. Res. Space Phys.* **125** e28033 (2020)
22. Makhmutov V S et al. *J. Atm. Sol.-Terr. Phys.* **149** 258 (2016)
23. Svirzhevskaya A K, Stozhkov Yu I, in *Trudy Vsesoyuznoi Konf. po Fizike Kosmicheskikh Luchei, Tashkent 1968* (Proc. of the All-Union Conf. on Cosmic Ray Physics, Tashkent, 1968) Pt. 2, Issue 3 (Moscow: FIAN, 1969) p. 63
24. Cliver E W, in *The Solar Activity Cycle: Physical Causes and Consequences* (Space Science Series of ISSI, Vol. 53, Eds A Balogh et al.) (New York: Springer, 2015) p. 169
25. Glette F et al., in *The Solar Activity Cycle: Physical Causes and Consequences* (Space Science Series of ISSI, Vol. 53, Eds A Balogh et al.) (New York: Springer, 2015) p. 35
26. Dolgoprudny Vernov Research Station. Laboratory of Solar and Cosmic Ray Physics. Lebedev Physical Institute, RAS, [https://sites.lebedev.ru/DNS\\_FIAN](https://sites.lebedev.ru/DNS_FIAN)
27. Parker E N *Interplanetary Dynamical Processes* (New York: Interscience Publ., 1963); Translated into Russian: *Dinamicheskie Protsessy v Mezhpplanetnoi Srede* (Translated from English edited by L I Dorman) (Moscow: Mir, 1965)
28. Potgieter M S, Vos E E *Astron. Astrophys.* **601** A23 (2017)
29. Tuska E B “Charge-sign dependent solar modulation of 1–10 GeV cosmic rays”, Ph.D. Thesis (Dissertation Abstracts Intern., Vol. 52-02, Sect. B, p. 0890) (Newark: Univ. of Delaware, 1990)
30. Rossi B, Olbert S *Introduction to the Physics of Space* (New York: McGraw-Hill, 1970); Translated into Russian: *Vvedenie v Fiziku Kosmicheskogo Prostranstva* (Moscow: Atomizdat, 1974)
31. Adriani O et al. *Astrophys. J.* **810** 142 (2015)
32. Aguilar M et al. *Phys. Rep.* **894** 1 (2021)
33. Stozhkov Yu I et al. *Bull. Russ. Acad. Sci. Phys.* **85** 1049 (2021); *Izv. Ross. Akad. Nauk Ser. Fiz.* **85** 1359 (2021)
34. Heber B et al. *Astrophys. J.* **699** 1956 (2009)
35. Nagashima K, in *Proc. of the 15th Intern. Cosmic Ray Conf., Plovdiv* Vol. 10 (Budapest: Dept. of Cosmic Rays, Central Research Inst. for Physics of the Hungarian Acad. of Sci., 1977) p. 380
36. Krymskii G F *Geomagn. Aeron.* **21** 923 (1981)
37. Cumming A C et al. *Astrophys. J.* **831** 18 (2016)
38. The Wilcox Solar Observatory, <http://wso.stanford.edu>
39. Mordvinov A V, Golovko A A, Yazev S A *Solnechno-Zemnaya Fizika* (Solar-Terrestrial Physics) Issue 25 (138) (Exec. Ed. A V Mikhalev) (Novosibirsk: Izd. SO RAN, 2014) p. 3